Aerospace Science and Technology 21 (2012) 55–63

Contents lists available at ScienceDirect

Aerospace Science and Technology

www.elsevier.com/locate/aescte

A sonic fix for ideal magnetogasdynamics equations using the Harten–Yee TVD scheme

Livio S. Maglione [a,*], Sergio A. Elaskar [b], Héctor H. Brito [c], Raúl A. Dean [a]

[a] Universidad Nacional de Río Cuarto, Fac. de Ingeniería, Río Cuarto, Ruta Nac. 36 Km. 601, X5804BYA, Córdoba, Argentina
[b] Universidad Nacional de Córdoba, Fac. de Ciencias Exactas Físicas y Naturales, Avenida Vélez Sársfield 299, Córdoba 5000, Argentina
[c] Instituto Universitario Aeronáutico, Av. Fuerza Aérea 6500, Córdoba 5010, Argentina

ARTICLE INFO

Article history:
Received 31 July 2010
Received in revised form 7 April 2011
Accepted 11 May 2011
Available online 25 May 2011

Keywords:
MGD
Riemann solver
TVD
PPT

ABSTRACT

Computational magnetogasdynamics (MGD) represents one of the most promising interdisciplinary computational technologies for aerospace design. However, the numerical techniques developed for the MGD equations must be able to solve correctly nonlinear hyperbolic differential equation system. In this work we present a modification of the original Harten–Yee scheme by incorporating a new sonic fix for the acoustic causality points using the finite volume technique. The proposed technique is used to simulate the coplanar MGD Riemann problem where results using the new sonic fix are compared with those given by the traditional Harten–Yee scheme. The obtained 2-D numerical results correctly satisfy the 1-D numerical solutions, and the oscillations present using the Harten–Yee traditional scheme, are reduced.

1. Introduction

The interaction between the flow of an electrically conducting medium and a magnetic field is a phenomenon with applications in aerospace, astrophysics, geophysics, interstellar gas masses dynamics, etc. [14,15,31]. Recent innovative aerodynamic designs modify the high-speed flow of an electrically conducting fluid by aerodynamic and electromagnetic field interactions [33]. The same phenomenon is used in aerospace application such as electric propulsion. This is presently being used for satellite orbit raising and station-keeping maneuvers. However, there are developments aimed to send electrically propelled spaceships to the Moon and Mars [6,13]. Electromagnetic plasma propulsion systems offer significantly higher exhaust velocities than chemical propulsion systems. The electric propulsion can be defined as the acceleration of gases for propulsion by electromagnetic means; according to the propulsive effects underlying physics, the electric thrusters can be grouped in three categories: electrothermal, electrostatic and electromagnetic.

Simulations of the physical processes occurring in the high density plasma that is ejected from the solid propellant surface in a small laser ablation thruster, are described in [25] using MACH2 code and [24] presents a one-dimensional hydrodynamic model of the atoms, electrons and ions used to solve the dynamics of a stationary plasma thruster. Argentine researchers are developing theoretical models and scientific software to solve the magnetogasdynamics (MGD) equations with the objective of applying it to a plasma thruster under construction in Argentina [4,9].

Magnetogasdynamics is an interdisciplinary area requiring the interplay of gasdynamics, electromagnetic field theory, ionized gas physics, chemical physics, and quantum physics [16,34,35]. A MGD model is generally based on the assumption that plasma can be regarded as a continuum and thus may be characterized by relatively few macroscopic quantities. A revision about the physical models used in aerospace applications is given in Ref. [7]. The MGD system is described by means of continuity, momentum, energy, and state equations. A full model (full magnetofluid dynamics equations—FMFD) for a flow affected by electromagnetic forces includes the full set of Maxwell's equations coupled with the Navier–Stokes equations. In the "simplified magnetofluid dynamics equations (SMFD)" or "magnetohydrodynamic approximation (MHD)", the Maxwell equations are replaced by the magnetic induction equation, which is still coupled to the Navier–Stokes equations. The real MGD equations constitute a parabolic–hyperbolic partial differential system. The parabolic part represents the non-ideal effects and it includes transport effects such as viscous and resistive diffusion and heat transfer. The hyperbolic or ideal part of the MGD equations presents non-convex singularities and the wave structure is more complicated than for the Euler equations [18]. The nonlinear coupling of these waves plays an important role in determining physical phenomenon and in the numerical solution [36].

The ideal MGD numerical simulations are a very important tool, by reducing expensive, and sometimes unviable, experimental

* Corresponding author. Tel.: +54 358 4676252, fax: +54 358 4676246.
E-mail addresses: smaglione@ing.unrc.edu.ar (L.S. Maglione), selaskar@efn.uncor.edu (S.A. Elaskar), hbrito@iua.edu.ar (H.H. Brito), rdean@ing.unrc.edu.ar (R.A. Dean).

1270-9638/$ – see front matter
doi:10.1016/j.ast.2011.05.005

Nomenclature

ρ	non-dimensional density	m	wave index
p	non-dimensional pressure	n	time level
$\boldsymbol{u}$	non-dimensional velocity vector	Δt	time step
$\boldsymbol{B}$	non-dimensional magnetic field vector	$\overline{\boldsymbol{F}}, \overline{\boldsymbol{G}}$	vector of numerical flux in the x, y directions
e	total non-dimensional energy density	$\boldsymbol{F}, \boldsymbol{G}$	vector of physical flux in the x, y directions
γ	specific heats ratio	$\boldsymbol{r}$	right eigenvectors of Jacobian fluxes
$\boldsymbol{W}$	vector of primitive variables	$\boldsymbol{l}$	left eigenvector of Jacobian fluxes
$\boldsymbol{U}$	vector of conservative variables	Φ	dissipation function
$[A_c]$	Jacobian of flux function in terms of conservative variables in the x direction	ψ	entropy correction function
i, j	mesh point locations in the x, y directions	α	wave strength

parametric studies. However, the numerical simulations always are limited by the ability to analyze and to solve accurately the hyperbolic nonlinear differential equation system.

To solve the ideal MGD equation system is convenient to use a conservative form. Then it is possible to implement numerical schemes for conservative equations which are also conservative and allow obtaining the correct jump conditions at discontinuities and shocks [20,36]. The utilization of the numerical conservative scheme is desirable because ensures that mass, momentum, and energy are indeed conserved. Several schemes has been proposed and implemented to solve the ideal MGD equations [1,26,38]; in this work, the Harten–Yee TVD (total variation diminishing) technique is used [40]. It has proven to be accurate and reliable for the simulation of supersonic flows of gases [10,12,41]. This technique is implemented here, with a modification, to numerically solve ideal MGD flows.

Among the difficulties to reach accurate numerical solutions for the ideal MGD equations, are the acoustic causality points where a new wave structure can be produced by the nonlinear wave interaction [5,19]. In ideal MGD the sonic points and the points where non-convexity appears, are points of acoustic causality [32]. In theses points it is necessary to apply a corrector entropy scheme introducing the necessary artificial viscosity.

In this paper we present a modification of the original Harten–Yee TVD scheme by incorporating a new sonic fix for the acoustic causality points. The proposed sonic fix is implemented by means of software specifically developed to solve the transient, two-dimensional ideal MGD equations. Finally, this software is used to simulate the Brio and Wu coplanar MGD Riemann problem [10] where results using the new sonic fix are compared with those given by the traditional Harten–Yee scheme.

2. Ideal magnetogasdynamics equations

The ideal MGD equations accurately describe the macroscopic dynamics of perfectly conducting plasma. This ideal MGD system expresses conservation of mass, momentum, energy, and magnetic flux and conforms a nonlinear conservative system of eight partial differential equations.

The equations of non-dimensional ideal one-fluid MGD in conservative form are given by [35]

$$\frac{\partial}{\partial t}\begin{bmatrix}\rho\\ \rho\boldsymbol{u}\\ \boldsymbol{B}\\ e\end{bmatrix}+\nabla\cdot\begin{bmatrix}\rho\boldsymbol{u}\\ \rho\boldsymbol{u}\boldsymbol{u}-\boldsymbol{B}\boldsymbol{B}+\boldsymbol{I}\left(p+\frac{1}{2}B^2\right)\\ \boldsymbol{u}\boldsymbol{B}-\boldsymbol{B}\boldsymbol{u}\\ \left(e+p+\frac{1}{2}B^2\right)\boldsymbol{u}-(\boldsymbol{B}\cdot\boldsymbol{u})\boldsymbol{B}\end{bmatrix}=\boldsymbol{0} \tag{1}$$

where ρ, $\boldsymbol{u}$, $\boldsymbol{B}$, e and p represent the mass density, the velocity vector, the magnetic field vector, the total energy and the pressure. The ninth equation that closes the system is the equation of state; for plasma that obeys the perfect gas equation the specific internal energy depends on temperature only. Substitution of the perfect gas state equation in the expression for the total energy produces

$$e=\frac{p}{\gamma-1}+\rho\frac{\boldsymbol{u}\cdot\boldsymbol{u}}{2}+\frac{\boldsymbol{B}\cdot\boldsymbol{B}}{2} \tag{2}$$

γ is the ratio between the specific heats.

By introducing a Cartesian coordinate system Eq. (1) can be written for two dimensions as

$$\frac{\partial\boldsymbol{U}}{\partial t}+\frac{\partial\boldsymbol{F}}{\partial x}+\frac{\partial\boldsymbol{G}}{\partial y}=\boldsymbol{0} \tag{3}$$

where the physical flux vectors are

$$\boldsymbol{F}=\begin{pmatrix}\rho u_x\\ \rho u_x^2-B_x^2+p+\frac{1}{2}B^2\\ \rho u_x u_y-B_xB_y\\ \rho u_x u_z-B_xB_z\\ 0\\ u_xB_y-u_yB_x\\ u_xB_z-u_zB_x\\ \left(e+p+\frac{1}{2}B^2\right)u_x-(\boldsymbol{B}\cdot\boldsymbol{u})B_x\end{pmatrix}$$

$$\boldsymbol{G}=\begin{pmatrix}\rho u_y\\ \rho u_x u_y-B_xB_y\\ \rho u_y^2-B_y^2+p+\frac{1}{2}B^2\\ \rho u_z u_y-B_zB_y\\ u_yB_x-B_yu_x\\ 0\\ u_yB_z-B_yu_z\\ \left(e+p+\frac{1}{2}B^2\right)u_y-(\boldsymbol{B}\cdot\boldsymbol{u})B_y\end{pmatrix} \tag{4}$$

and the vector of conservative variables $\boldsymbol{U}$ is

$$\boldsymbol{U}=(\rho,\rho u_x,\rho u_y,\rho u_z,B_x,B_y,B_z,e)^T \tag{5}$$

Eq. (3) can be written in the quasi-linear form as

$$\frac{\partial\boldsymbol{U}}{\partial t}+[A_c]\frac{\partial\boldsymbol{U}}{\partial x}+[B_c]\frac{\partial\boldsymbol{U}}{\partial y}=\boldsymbol{0} \tag{6}$$

where $[A_c]$, $[B_c]$ are the Jacobian matrices in terms of conservative variables. The evaluation of the eigenvalues and the eigenvectors is simpler using the conservative variables:

$$\boldsymbol{W}=(\rho,u_x,u_y,u_z,B_x,B_y,B_z,p)^T \tag{7}$$

In the system given by Eq. (6) each Jacobian matrix has a null eigenvalue. To overcome this restriction the eight-wave technique

introduced by Powell [28] is used in this work and the eigenvectors are normalized according to Zachary et al. [42] and Roe and Balsara [29]. The expressions resulting for the eigenvalues and eigenvectors are:

- entropy wave $\lambda^1 = u_x$

$$\boldsymbol{r}_e = \begin{Bmatrix} 1 \\ 0 \\ 0 \\ 0 \\ 0 \\ 0 \\ 0 \\ 0 \end{Bmatrix} \qquad \boldsymbol{l}_e = \begin{Bmatrix} 1 \\ 0 \\ 0 \\ 0 \\ 0 \\ 0 \\ 0 \\ -\frac{1}{c^2} \end{Bmatrix} \tag{8}$$

- Alfvén waves $\lambda^2, \lambda^3 = u_x \pm \frac{|B_x|}{\sqrt{\rho}}$

$$\boldsymbol{r}_a^{\pm} = \frac{1}{\sqrt{2}} \begin{Bmatrix} 0 \\ 0 \\ -\beta_z \\ \beta_y \\ 0 \\ \pm\sqrt{\rho}\beta_z \\ \mp\sqrt{\rho}\beta_y \\ 0 \end{Bmatrix} \qquad \boldsymbol{l}_a^{\pm} = \frac{1}{\sqrt{2}} \begin{Bmatrix} 0 \\ 0 \\ -\beta_z \\ \beta_y \\ 0 \\ \pm\frac{\beta_z}{\sqrt{\rho}} \\ \mp\frac{\beta_y}{\sqrt{\rho}} \\ 0 \end{Bmatrix} \tag{9}$$

- fast magneto-acoustic waves

$$\lambda^4, \lambda^5 = u_x \pm \sqrt{\tfrac{1}{2\rho}\left[\gamma p + \boldsymbol{B}\cdot\boldsymbol{B} + \sqrt{(\gamma p + \boldsymbol{B}\cdot\boldsymbol{B})^2 - 4\gamma p B_x^2}\right]}$$

$$\boldsymbol{r}_f^{\pm} = \begin{Bmatrix} \rho\alpha_f \\ \pm\alpha_f c_f \\ \mp\alpha_s c_s \beta_y \operatorname{sgn}(B_x) \\ \mp\alpha_s c_s \beta_z \operatorname{sgn}(B_x) \\ 0 \\ \alpha_s\sqrt{\rho} c \beta_y \\ \alpha_s\sqrt{\rho} c \beta_z \\ \alpha_f \gamma p \end{Bmatrix} \qquad \boldsymbol{l}_f^{\pm} = \begin{Bmatrix} 0 \\ \pm\frac{\alpha_f c_f}{2c^2} \\ \mp\frac{\alpha_s}{2c^2} c_s \beta_y \operatorname{sgn}(B_x) \\ \mp\frac{\alpha_s}{2c^2} c_s \beta_z \operatorname{sgn}(B_x) \\ 0 \\ \frac{\alpha_s}{2\sqrt{\rho}c}\beta_y \\ \mp\frac{\alpha_s}{2\sqrt{\rho}c}\beta_z \\ \frac{\alpha_f}{2\rho c^2} \end{Bmatrix} \tag{10}$$

- slow magneto-acoustic waves

$$\lambda^6, \lambda^7 = u_x \pm \sqrt{\tfrac{1}{2\rho}\left[\gamma p + \boldsymbol{B}\cdot\boldsymbol{B} - \sqrt{(\gamma p + \boldsymbol{B}\cdot\boldsymbol{B})^2 - 4\gamma p B_x^2}\right]}$$

$$\boldsymbol{r}_s^{\pm} = \begin{Bmatrix} \rho\alpha_s \\ \pm\alpha_s c_s \\ \pm\alpha_f c_f \beta_y \operatorname{sgn}(B_x) \\ \pm\alpha_f c_f \beta_z \operatorname{sgn}(B_x) \\ 0 \\ -\alpha_f\sqrt{\rho} c \beta_y \\ -\alpha_f\sqrt{\rho} c \beta_z \\ \alpha_s \gamma p \end{Bmatrix} \qquad \boldsymbol{l}_s^{\pm} = \begin{Bmatrix} 0 \\ \pm\frac{\alpha_s c_s}{2c^2} \\ \pm\frac{\alpha_f}{2c^2} c_f \beta_y \operatorname{sgn}(B_x) \\ \pm\frac{\alpha_f}{2c^2} c_f \beta_z \operatorname{sgn}(B_x) \\ 0 \\ -\frac{\alpha_f}{2\sqrt{\rho}c}\beta_y \\ \frac{\alpha_f}{2\sqrt{\rho}c}\beta_z \\ \frac{\alpha_s}{2\rho c^2} \end{Bmatrix} \tag{11}$$

- magnetic flux wave $\lambda^8 = u_x$

$$\boldsymbol{r}_d = \begin{Bmatrix} 0 \\ 0 \\ 0 \\ 0 \\ 1 \\ 0 \\ 0 \\ 0 \end{Bmatrix} \qquad \boldsymbol{l}_d = \begin{Bmatrix} 0 \\ 0 \\ 0 \\ 0 \\ 1 \\ 0 \\ 0 \\ 0 \end{Bmatrix} \tag{12}$$

where

$$c = \sqrt{\gamma\frac{p}{\rho}} \qquad c_{f,s}^2 = \frac{1}{2}\left(\frac{\gamma p + B^2}{\rho} \pm \sqrt{\left(\frac{\gamma p + B^2}{\rho}\right)^2 - 4\frac{\gamma p B_x^2}{\rho^2}}\right)$$

$$c_A = \frac{|B_x|}{\sqrt{\rho}} \tag{13}$$

$$\alpha_f^2 = \frac{c^2 - c_s^2}{c_f^2 - c_s^2} \qquad \alpha_s^2 = \frac{c_f^2 - c^2}{c_f^2 - c_s^2}$$

$$\operatorname{sgn}(x) = \begin{cases} 1 & \text{if } x \geqslant 0 \\ -1 & \text{otherwise} \end{cases} \tag{14}$$

$$\beta_y = \begin{cases} \dfrac{B_y}{B_\perp} & B_\perp \neq 0 \\ \dfrac{1}{\sqrt{2}} & B_\perp = 0 \end{cases} \qquad \beta_z = \begin{cases} \dfrac{B_z}{B_\perp} & B_\perp \neq 0 \\ \dfrac{1}{\sqrt{2}} & B_\perp = 0 \end{cases}$$

$$\beta_\perp = \sqrt{B_y^2 + B_z^2} \tag{15}$$

The characteristic velocity λ_i defines a characteristic field. Sometimes one also speaks of the $\boldsymbol{R}^i$-field, that is the characteristic field defined by the right eigenvectors. A λ_i-characteristic field is said to be linearly degenerate if

$$\nabla\lambda_i(\boldsymbol{U})\cdot\boldsymbol{r}^i(\boldsymbol{U}) = 0 \quad \forall \boldsymbol{U} \in \Re^m \tag{16}$$

A λ_i-characteristic field is said to be genuinely nonlinear if

$$\nabla\lambda_i(\boldsymbol{U})\cdot\boldsymbol{r}^i(\boldsymbol{U}) \neq 0 \quad \forall \boldsymbol{U} \in \Re^m \tag{17}$$

The Alfvén waves, the entropy wave and the magnetic flux wave, are linearly degenerate fields; hence the wave velocity is constant throughout the wave. The slow and fast characteristic fields are genuinely nonlinear. However, these fields under particular relations between the magnetic field, the sound velocity and the Alfvén velocity; are non-convex characteristic fields [32].

3. Numerical method

This section presents the technique used to obtain the numerical solution of the PDE system described by Eq. (1). A finite volume scheme has been implemented using a structured mesh. An approximate Riemann solver is utilized to calculate the fluxes with an explicit finite-differences scheme for the time evolution.

The numerical fluxes are evaluated by means of the Harten–Yee TVD technique, which correctly allows the capturing of discontinuities, simultaneously achieving a second-order approach. This scheme was developed by gasdynamics equations [40] and latter was implemented for MGD equations [38].

In the context of shock-capturing MHD codes, three approaches became rather popular to handle the $\nabla\cdot\boldsymbol{B} = 0$ constraint. All three approaches can be regarded as some modification of, or addition to a base scheme. The base scheme can be, for example, Harten's TVD [17]. The three approaches differ in how the base scheme is modified regarding the induction equation. The first approach is the eight-wave formulation of the MHD equations suggested by Powell [28], the second approach was named constrained transport (CT) by Evans and Hawley [11] and the third approach is

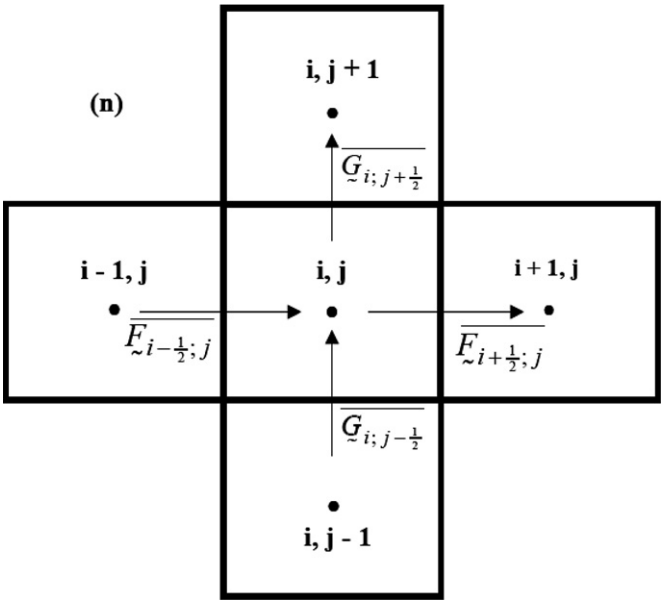

Fig. 1. Five adjacent cells of the two-dimensional domain.

the projection scheme, which, in the context of MHD, was first suggested by Brackbill and Barnes [2]. In this paper we use the first approach. Tóth in [37] compared seven schemes to maintain $\nabla \cdot \boldsymbol{B} = 0$ constraint numerically and showed that, the average error is the smallest for the eight-wave and projection schemes in the solution of 2.5 D MGD shock tube test. Also showed the eight-wave is found to behave better in terms of stability and accuracy than the discretization of the usual conservative form.

The explicit TVD-finite volume scheme can be expressed as, see Fig. 1,

$$\boldsymbol{U}_{ij}^{n+1} = \boldsymbol{U}_{ij}^{n} - \Delta t\left[\frac{\overline{\boldsymbol{F}}_{i+\frac{1}{2};j}^{n} - \overline{\boldsymbol{F}}_{i-\frac{1}{2};j}^{n}}{\Delta x} + \frac{\overline{\boldsymbol{G}}_{i;j+\frac{1}{2}}^{n} - \overline{\boldsymbol{G}}_{i;j-\frac{1}{2}}^{n}}{\Delta y}\right] \tag{18}$$

where n, Δt, (i, j) are the time level, the time step, and the mesh point locations in the x, y directions. The function that determines the second-order numerical flux $\bar{F}$ is defined as [38]

$$\overline{\boldsymbol{F}}_{i+\frac{1}{2};j}^{n} = \frac{1}{2}\left(\boldsymbol{F}_{i+1}^{n} + \boldsymbol{F}_{i}^{n} + \left(\sum_{m} \boldsymbol{r}_{i+\frac{1}{2}}^{m} \Phi_{i+\frac{1}{2}}^{m}\right)^{(n)}\right) \tag{19}$$

where m, $\boldsymbol{r}^m$, Φ are the wave index, the right eigenvectors of Jacobian matrix and the dissipation function. The latter is defined as

$$\Phi_{i+\frac{1}{2}}^{m} = \left(g_{i+1}^{m} + g_{i}^{m}\right) - \psi\left(\lambda_{i+\frac{1}{2}}^{m} + \gamma_{i+\frac{1}{2}}^{m}\right)\alpha_{i+\frac{1}{2}}^{m} \tag{20}$$

Here g is the limiter function, ψ the entropy correction function and α the wave strength. In this work the limiter function used is one of minmod type,

$$g_{i}^{m} = \operatorname{sgn}\left(\lambda_{i+\frac{1}{2}}^{m}\right)\max\left\{0, \min\left[\sigma_{i+\frac{1}{2}}^{m}\left|\alpha_{i-\frac{1}{2}}^{m}\right|, \sigma_{i-\frac{1}{2}}^{m}\frac{\operatorname{sgn}(\lambda_{i+1/2}^{m})}{2}\alpha_{i-\frac{1}{2}}^{m}\right]\right\}$$

$$\sigma_{i+\frac{1}{2}}^{m} = \sigma\left(\lambda_{i+\frac{1}{2}}^{m}\right) \tag{21}$$

$$\gamma_{i+\frac{1}{2}}^{m} = \begin{cases} \dfrac{1}{\alpha_{i+\frac{1}{2}}^{m}}\left(g_{i+1}^{m} - g_{i}^{m}\right) & \alpha_{i+\frac{1}{2}}^{m} \neq 0 \\ 0 & \alpha_{i+\frac{1}{2}}^{m} = 0 \end{cases} \tag{22}$$

For time-accurate calculations in explicit numerical algorithms

$$\sigma(z) = \frac{1}{2}\left[\psi(z) - \frac{\Delta t}{\Delta x}z^2\right] \tag{23}$$

The wave strength of the m-th wave is calculated as

$$\alpha^{m} = \boldsymbol{l}_{p}^{m} \cdot (\boldsymbol{W}_{i+1} - \boldsymbol{W}_{i}) \tag{24}$$

An approximate Roe-type Riemann solver, as indicated in Eqs. (19)–(24), produces only shock waves so that a rarefaction shock wave replaces a smooth rarefaction wave. A rarefaction shock wave violates the entropy condition generating a non-physical solution. To overcome this intrinsic problem of the Roe schemes is introduced a "sonic entropy fix" that smoothes out eigenvalues in the vicinity of the sonic point [36]. Harten [17] suggested an entropy fix for Roe's method, which has widespread use for gasdynamics equations:

$$\psi(z) = \begin{cases} |z| & |z| \geqslant \delta \\ \dfrac{1}{2\delta}\left(z^2 + \delta^2\right) & |z| < \delta \end{cases} \tag{25}$$

The function ψ in Eq. (25) is an entropy correction to z, whereas δ is generally a small and constant value that needs to be calibrated for each problem. A proper choice of the entropy parameter δ for higher Mach number flows not only helps in preventing non-physical solutions but can act, in some sense, as a control in the convergence rate and in the sharpness of shocks [41].

4. Results and discussion

To assess accuracy and reliability in computational simulations at first stage of research, after development and implementation the code was subjected to several tests with emphasis in the verification of the results. The verification and validation concepts (V&V) are consistent with the American Institute of Aeronautics and Astronautics (AIAA) definitions, i.e., verification as the process of determining that a model implementation accurately represents the developer's conceptual description of the model and the solution to the model, and Validation as the process of determining the degree to which a model is an accurate representation of the real world from the perspective of the intended uses of the model [27].

The code was first evaluated through solving the 1-D MGD case [8]. Then, the software ability to solve 2-D gasdynamics problems was evaluated, and the results were found to agree with the analytical solution [22]. Finally, the Riemann problem introduced by Brio and Wu was considered as a "benchmark" [3] and the correct behavior of the software in 2-D magnetogasdynamics problems was verified. The proposed MGD Riemann problem has not analytical solutions but numerical solutions were obtained by other researches [3,30,38].

Numerical results of the MGD Riemann problem using different alternatives are presented in this section. For MGD flows, this benchmark is called coplanar Riemann problem. This problem initially has a discontinuity that separates two constant states, a leftward one and a rightward one. These states are defined by the corresponding initials conditions. With the purpose of verifying the correct operation of the 2-D code being presented here, the mesh is rotated with respect to the longitudinal axis of the flow. The code is thus forced to simulate a 2-D flow.

The initial conditions used in the simulation are:

$$W_l = (1.0, 0.0, 0.0, 0.0, 0.75, 1.0, 0.0, 1.0)^T$$
$$W_r = (0.125, 0.0, 0.0, 0.0, 0.75, -1.0, 0.0, 0.1)^T \tag{26}$$

The traditional Harten–Yee scheme, that was developed for gasdynamics equations, was applied to Eq. (1) using the sonic fix,

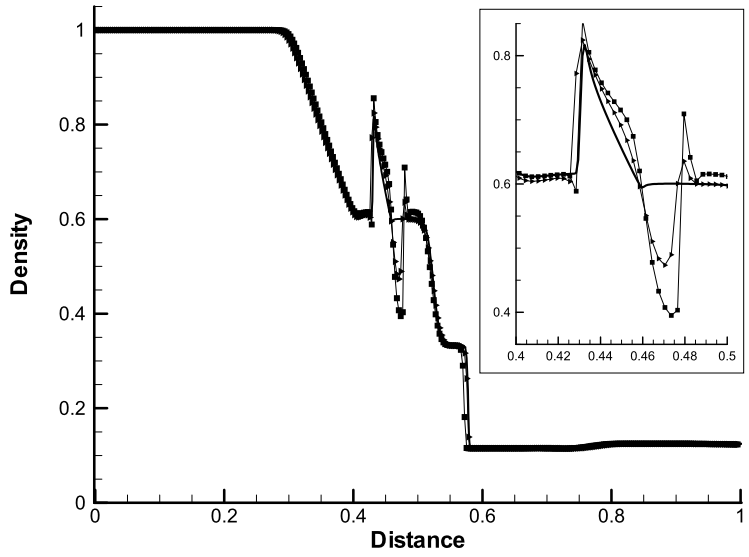

(a)

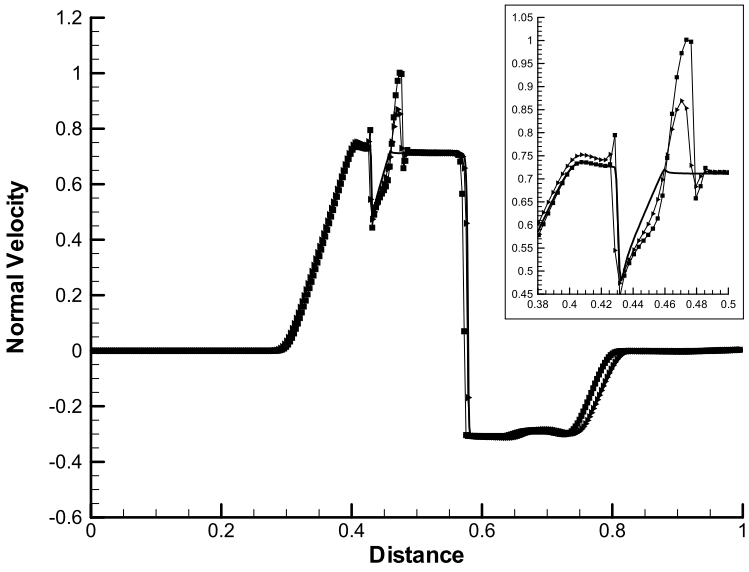

(b)

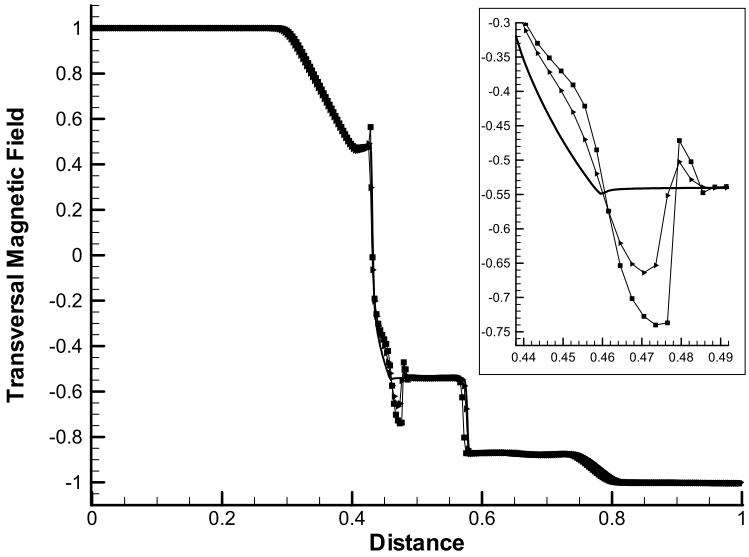

(c)

Fig. 2. (a) Density for 2-D MGD Riemann problem. (b) Normal velocity for 2-D MGD Riemann problem. (c) Transversal magnetic field for 2-D MGD Riemann problem. Solid line: benchmark 1D, square: Harten–Yee technique with $\delta = 1E{-}3$, right triangle: Harten–Yee and Van Leer technique.

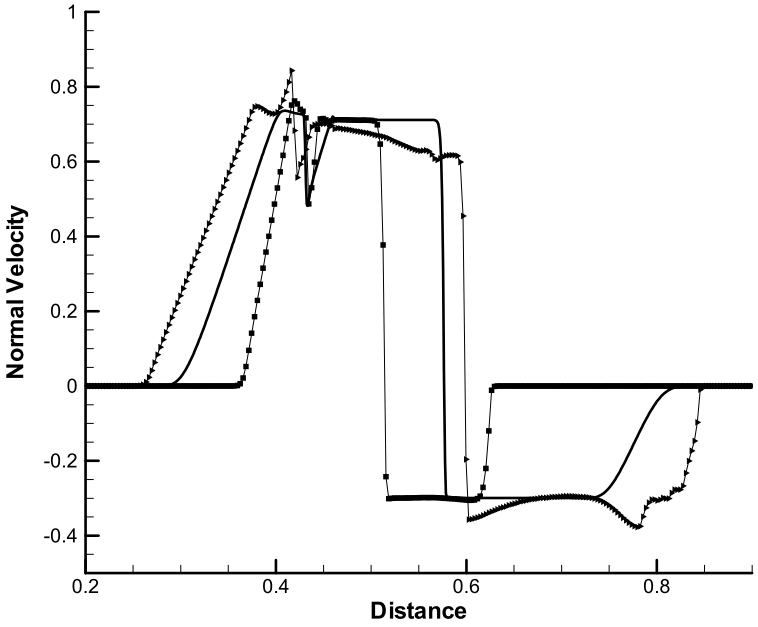

Fig. 3. Normal velocity for 2-D MGD Riemann problem. Solid line: benchmark 1D, square and right triangle: H–Y technique with average δ for different times.

given by Eq. (25). This sonic fix acts only on sonic point, but it does not act on non-convex point; because the gasdynamics equations do not present non-convex points. Fig. 2 shows the results by the Brio and Wu benchmark applying the Harten–Yee scheme with $\delta = 0.001$. It stands from the figure that large oscillations occur around the compound wave; these oscillations destabilize the numerical simulations and prevent to find solutions for relatively long times.

To obtain "proper" numerical results for the Brio and Wu 2-D MGD problem, the entropy correction of Harten scheme, Eq. (25), needs to be calibrated with relatively big values of δ [23]. For gasdynamics hypersonic flows, a constant or a variable δ was found to be insufficient, but a variable δ depending on the spectral radius of the Jacobian matrices is very helpful in terms of stability and convergence rate [41]. Numerical experiments show that the technique of the spectral radius of the Jacobian matrices does not provide good results on the Brio and Wu 2-D MGD problem [3]. The use of a constant value, for 2-D simulations, equal to the average in absolute value of the eigenvalues of the Jacobian matrices shows satisfactory results for short time [21,23], however this technique forces the method to introduce too much numerical viscosity around a big vicinity of the sonic points. As a result of this scheme the solutions are not particularly satisfactory for long computation time, especially in capturing the fast shock wave moving to the right (see Fig. 3).

In order to obtain a method that does not need δ calibration for each MGD problem, it is convenient to improve the Van Leer technique [39], widely applied for gases.

$$\delta_{GD} = \max\left[\left|\lambda^m_{i+\frac{1}{2}} - \lambda^m_{i-\frac{1}{2}}\right|, 0\right] \tag{27}$$

$$\delta^{MGD}_k = \begin{cases} \max\left[\left|\lambda^m_{i+\frac{1}{2}} - \lambda^m_{i-\frac{1}{2}}\right|\right] & \text{if } \lambda^m_{i+\frac{1}{2}} \text{ cuts across zero} \\ \min\left|\lambda^m_{i+\frac{1}{2}}\right| & \text{otherwise} \end{cases}$$

$$\text{with } k = 1, \ldots, 8 \tag{28}$$

As an alternative we have implemented the traditional Harten–Yee technique only in sonic points, but δ defined by Eq. (28). The results are shown in Fig. 2; we can observe that the results have more accuracy and the oscillations have been reduced. Table 1 shows, for two time values, the eigenvalues that cross over

Table 1
Numerical values of δ for two different times and the eigenvalues that cross over zero.

Wave m	$\max[\lvert\lambda^m_{i+\frac{1}{2}} - \lambda^m_{i-\frac{1}{2}}\rvert]$			Zero-crossings		
	Case			Case		
	1D x	2D x	2D y	1D x	2D x	2D y
			$t = 0.03077$			
1 and 8	0.262	0.341	0.104	Yes	Yes	Yes
2	0.147	0.275	0.194	No	No	Yes
3	0.512	0.677	0.090	No	Yes	No
4	0.187	0.316	0.223	No	No	No
5	0.684	0.746	0.079	No	Yes	No
6	0.348	0.438	0.105	No	No	Yes
7	0.176	0.244	0.103	No	Yes	No
			$t = 0.08081$			
1 and 8	0.259	0.356	0.103	Yes	Yes	Yes
2	0.145	0.527	0.192	No	No	Yes
3	0.491	0.700	0.109	No	Yes	No
4	0.190	0.600	0.237	No	No	No
5	0.656	0.762	0.119	No	Yes	No
6	0.343	0.456	0.104	No	No	Yes
7	0.175	0.342	0.103	No	Yes	No

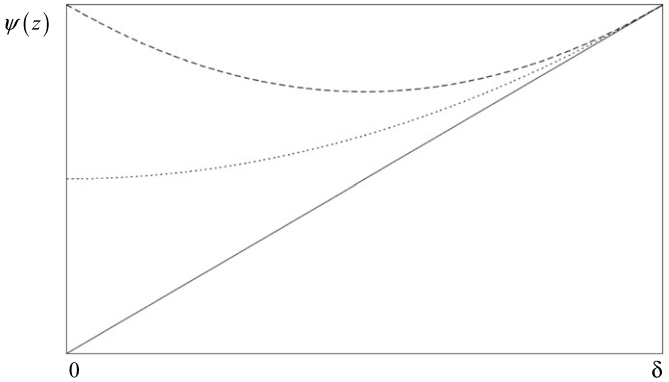

Fig. 4. Comparison between the new sonic fix and Harten's original (dotted line: original sonic fix, long dash line: proposed sonic fix).

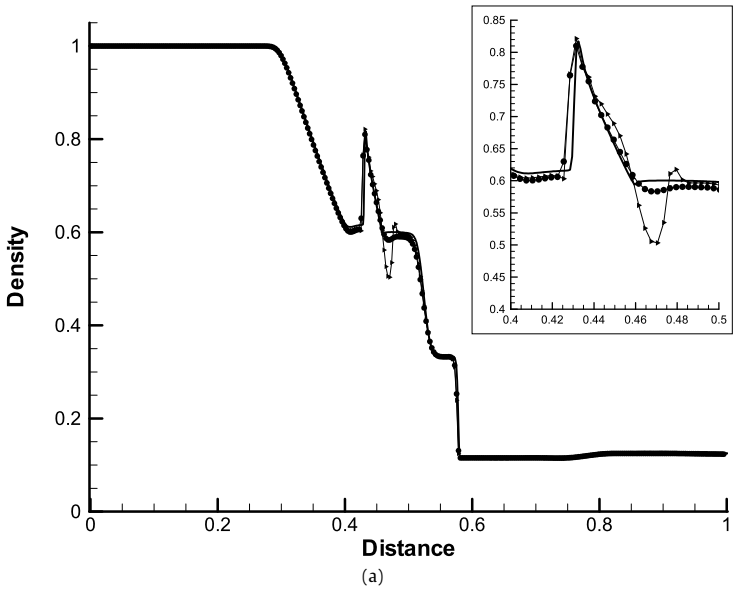

(a)

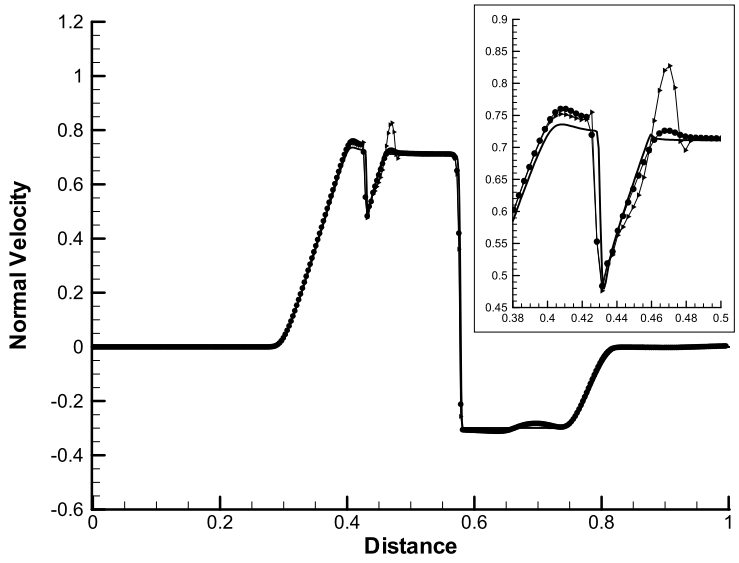

(b)

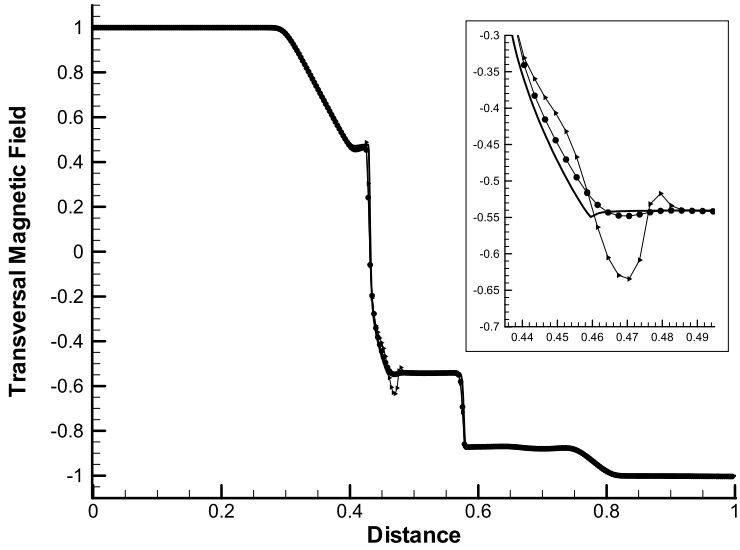

(c)

Fig. 5. (a) Density for 2-D MGD Riemann problem. (b) Normal velocity for 2-D MGD Riemann problem. (c) Transversal magnetic field for 2-D MGD Riemann problem. Solid line: benchmark 1D, square: new technique implemented in all acoustic points, right triangle: new technique implemented only in non-convex points.

Table 2
Numerical errors in the normal magnetic field.

	H–Y technique with $\delta = 1E{-}3$	New function, Eq. (29), and δ by Eq. (28)
ϵ_{max}	0.0743	0.016
ϵ_{ave}	0.00396	0.00359

zero and the values of δ, Eq. (28), when the modified Van Leer's technique is used for the magnetogasdynamic problem of Brio and Wu [3]. It can also been observed that in the two-dimensional case, more zero crossings appear than for the one-dimensional case. This situation is particularly important in the compound wave (7-th). To include the treatment of non-convex points in the numerical method, we have implemented Eq. (25) together with δ as given by Eq. (28) for all acoustic points; however, we found convergence difficulties.

For increasing the accuracy obtained with the previous schemes and to avoid the spurious oscillations, a new entropy correction function is proposed so that greater numerical viscosity only restricted to the proximity of the acoustic points can be achieved,

$$\psi(z) = \begin{cases} |z| & \text{others} \\ \dfrac{z^2}{\delta^2} + \dfrac{\delta - 2}{\delta}|z| + 1 & \text{acoustic points} \end{cases} \tag{29}$$

Although the correction is applied not only in sonic points but also non-convex points, we keep the terminology "sonic fix" for the entropy correction function, to be widely used in the simulation of gas flows.

A comparison between Harten's original sonic entropy fix, Eq. (25), and the new proposed fix, Eq. (20), is shown in Fig. 4. This new function, Eq. (29), is a continuously differentiable approximation to $|z|$, fulfilling

$$\begin{aligned} &\psi(\delta)_{\delta^-} = \psi(\delta)_{\delta^+} \\ &\psi(0)_{\delta^-} = 1 \\ &\left.\frac{d\psi(z)_{\delta^-}}{dz}\right|_{z=\delta} = \left.\frac{d\psi(z)_{\delta^+}}{dz}\right|_{z=\delta} \end{aligned} \tag{30}$$

Firstly this new function was implemented only for non-convex points, whereas for sonic points Eq. (25) was used; for both types of points δ was evaluated according to Eq. (28). Under these conditions we can reach convergence and the results are presented in Fig. 5, although the oscillations hardly show a slight reduction.

Finally we have applied in all acoustic points the new function given by Eq. (29) together with δ calculated by Eq. (28). The results are shown in Fig. 5. We stress that the oscillations were significantly reduced around the compound wave. In the problem of Brio and Wu 2-D MGD theoretical solution for the normal magnetic field is a constant value equal to 0.75, while the numerical solution are variations around 0.75. For a quantitative comparison of the various schemes handling the $\nabla \cdot \boldsymbol{B} = 0$ constraint is usual to calculate the numerical error in the normal magnetic field [37]. The maximum relative error of a variable u on an $N \times M$ mesh, is defined as

$$\epsilon_{\max} = \frac{\max[|u_{i,j}^{\text{Aprx}} - u_{i,j}^{\text{Theor}}|]}{|u_{(i,j)_{\max}}^{\text{Theor}}|} \tag{31}$$

and the average relative error,

$$\epsilon_{\text{ave}} = \frac{\sum_{i=1}^{N}\sum_{j=1}^{M}|u_{i,j}^{\text{Aprx}} - u_{i,j}^{\text{Theor}}|}{\sum_{i=1}^{N}\sum_{j=1}^{M}|u_{i,j}^{\text{Theor}}|} \tag{32}$$

where Aprx corresponds to the numerical solution and Theor to an analytic solution or absence of a high resolution numerical solution. Table 2 shows the numerical errors in the normal magnetic field with the techniques presented previously; the scheme presented in this work satisfies more accurately the condition $\nabla \cdot \boldsymbol{B} = 0$ that the traditional Harten–Yee scheme. Also highlights

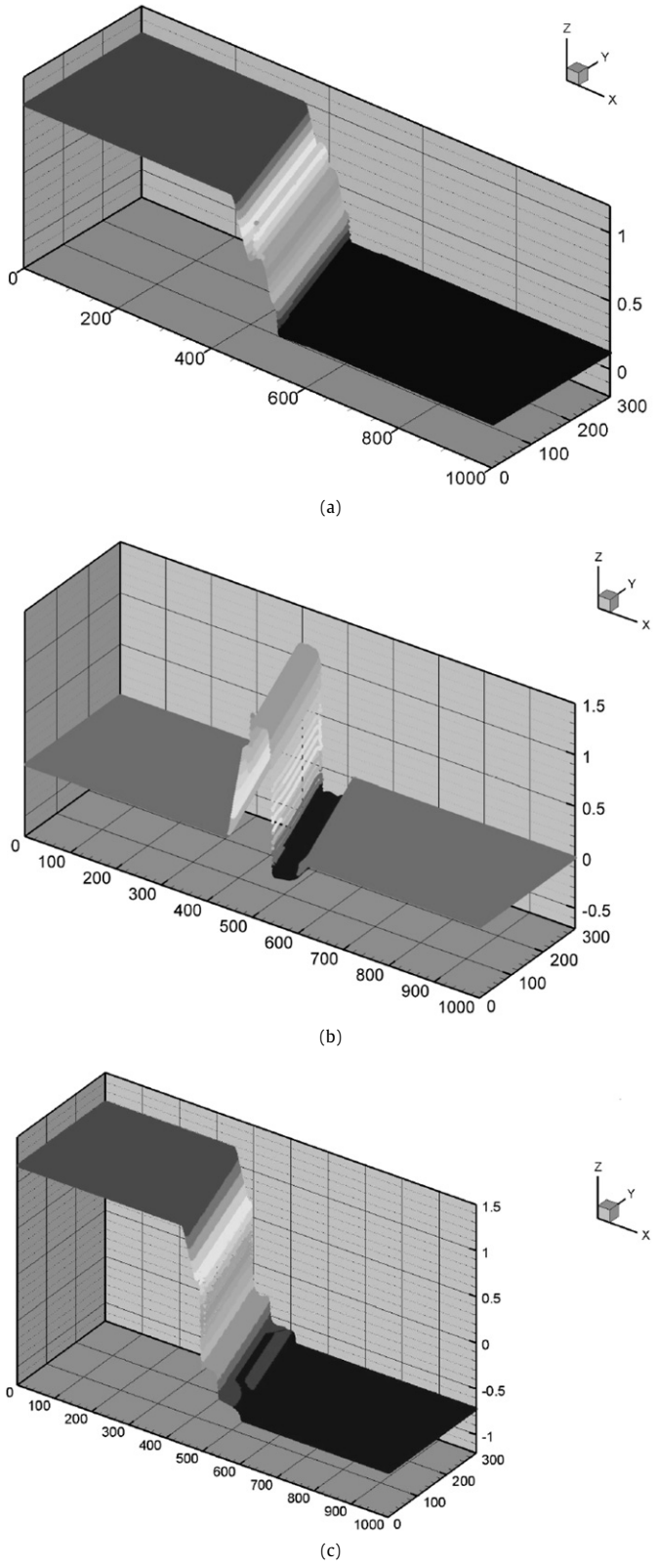

Fig. 6. (a) Density in 2-D MGD Riemann problem. (b) Component x of the velocity vector for the 2-D MGD Riemann problem. (c) Component y of the magnetic field vector for the 2-D MGD Riemann problem.

that the error introduced by the new scheme is significantly less than that given in Ref. [37].

At the present stage of development, the entropy parameter seems still highly geometric and problem dependent. A universal method is yet to be discovered. However, we note that the joint implementation of Eqs. (28) and (29) has proven to be an effective method for the magnetogasdynamic Riemann problem.

Fig. 6 shows the density, the x component of the velocity vector and the y component of the magnetic field vector obtained with the joint implementation of Eqs. (28) and (29). The waves present in MGD flows are visible in the picture.

5. Conclusion

The modification of Harten and Yee's original method presented in this work, incorporating a new sonic fix, has proven reliable through verification by using a very demanding benchmark (2-D magnetogasdynamic shock tube constitutes a well known test case to evaluate the behavior of numerical codes).

The obtained 2-D numerical results correctly satisfy the 1-D numerical solutions already published. The oscillations, present when using Harten–Yee traditional scheme, are notably reduced and the new sonic fix is applied in sonic and non-convex points. This new technique has two important advantages:

- The method does not need particular calibration.
- The method increases the numerical viscosity in the proximity of the acoustic points, only.

The next objective of this research is to develop a 3-D, non-steady magnetogasdynamics numerical code using non-structured meshes and finite volumes. In a near future, the objective is to achieve the capability of simulating flows for plasma propulsion in complex geometries.

Acknowledgements

This work was supported by the Science and Technology Office of the National University of Rio Cuarto (SECyT-UNRC), the National Agency for the Support of Science and Technology (ANPCyT-Argentina) and CONICET.

References

[1] J. Balbas, E. Tadmor, C. Wu, Non-oscillatory central schemes for one and two dimensional MHD equations, J. Comput. Phys. 201 (1) (2004) 261–285.
[2] J. Brackbill, D. Barnes, The effect of nonzero $\nabla \cdot \boldsymbol{B}$ on the numerical solution of the magnetohydrodynamic equations, J. Comput. Phys. 35 (1980) 426.
[3] M. Brio, C. Wu, An upwind differencing scheme for the equations of magnetohydrodynamics, J. Comput. Phys. 45 (1988) 400–422.
[4] H.H. Brito, S.A. Elaskar, L.S. Maglione, R.A. Dean, R. Duelli, Concept study of a solid propellant magnetoplasmadynamic microthruster, in: Proc. 57th International Astronautical Congress IAC, Valencia, Spain, 2006, IAC-06-C4.P.4.09.
[5] R. Courant, K. Friedrich, Supersonic Flow and Shock Waves, Springer, New York, 1999.
[6] F. Currant, Electric propulsion activities in U.S. industry, in: Proc. 26th International Electric Propulsion Conference, Kitakyushu, Japan, 1999, IEPC-99-01.
[7] D. D'Ambrosio, D. Giordano, Electromagnetic flows dynamics for aerospace applications. Part I: Classification and critical review of physical models, in: Proc. 35th AIAA Plasmadynamics and Laser Conference, 2004, Paper 2004-2165.
[8] S.A. Elaskar, H.H. Brito, Numerical solution of the magnetogasdynamics equations as a tool for the design of pulsed plasma thruster, in: Proc. International Electric Propulsion Conference 2001, Pasadena, USA, 2001, IEPC-01-141.
[9] S.A. Elaskar, L.S. Maglione, O. Falcinelli, H.H. Brito, J. Tamagno, Numerical simulation of MGD flows for plasma propulsion, in: Proc. 52nd International Astronautical Congress IAC, Toulouse, France, 2001, IAC-01-S.4.03.
[10] S.A. Elaskar, H.H. Brito, J. Tamagno, Numerical simulation of high enthalpy pulse facilities as an exploratory tool for PPT's modeling, in: Proc. 51st International Astronautical Congress, Río de Janeiro, Brazil, 2000, IAF-00-S.4.10.
[11] C.R. Evans, J.F. Hawley, Simulation of magnetohydrodynamic flows: A constrained transport method, Astrophys. J. 332 (1988) 659.
[12] O. Falcinelli, S.A. Elaskar, J. Tamagno, Reducing the numerical viscosity in non-structured three-dimensional finite volumes computations, J. Spacecr. Rockets 45 (2) (2008) 406–408.
[13] J. Gilland, D. Fiehler, V.J. Lyons, Electric propulsion concepts enabled by high power systems for space exploration, NASA/TM – 2005-213371, 2005.
[14] D. Giordano, Hypersonic flow governing equations with electromagnetic fields, in: Proc. 33rd Plasmadynamics and Lasers Conference, Maui, Hawaii, EEUU, 2002, AIAA Paper 2002-2165.
[15] J.P. Goedbloed, R. Keppens, S. Poedts, Advanced Magnetohydrodynamics with Applications to Laboratory and Astrophysical Plasmas, Cambridge University Press, New York, 2010.
[16] R. Goldston, P. Rutherford, Introduction to Plasma Physics, Institute of Physics Publishing, London, 2003.
[17] A. Harten, High resolution schemes for hyperbolic conservation laws, Courant Mathematics and Computing Laboratory, U.S. Department of Energy, 1982, DOE/ER/03077-175.
[18] A.R. Kantrowitz, H.E. Petschek, MHD Characteristics and Shock Waves, Plasma Physics in Theory and Application, McGraw–Hill, New York, 1966.
[19] R.J. Leveque, D. Milhalas, E.A. Dorfi, E. Muller, Computational Methods for Astrophysical Fluid Flow, Springer, Germany, 1998.
[20] R.J. Leveque, Numerical Methods for Conservation Law, Birkhäuser Verlag, 1992.
[21] L.S. Maglione, et al., A software engineering for numerical simulation of 2-D non-stationary real MGD flows, PAMM J. 7 (1) (2007) 2010027–2010028.
[22] L.S. Maglione, S.A. Elaskar, H.H. Brito, Simulación 2-D de flujos supersónicos de plasmas y gases, in: Proc. Congreso Argentino de Tecnología Espacial 2003, Neuquén, Argentina, 2003.
[23] L.S. Maglione, S.A. Elaskar, H.H. Brito, Numerical simulation of two-dimensional, non-steady, ideal magnetogasdynamic equations, in: Proc. 28th International Electric Propulsion Conference IEPC, Toulouse, France, 2003, Paper No. 70.
[24] M. Mirshams, et al., Hydrodynamic simulation of a stationary plasma thruster in steady state regime, Aerospace Sci. Tech. 13 (2009) 402–405.
[25] T. Moeller, Y.-K. Chang, MACH2 simulations of a micro laser ablation plasma thruster, Aerospace Sci. Tech. 11 (2007) 481–489.
[26] R.S. Myong, P.L. Roe, On Godunov-type schemes for magnetohydrodynamics: 1. A model system, J. Comput. Phys. 147 (2) (1998) 545–567.
[27] W.L. Oberkampf, T. Truncano, Verification and validation in computational fluid dynamics, Prog. Aerospace Sci. 38 (2002) 209–272.
[28] K. Powell, An approximate Riemann solver for magnetohydrodynamics (that works in more than one dimension), NASA Contract No. NAS1-19480, 1995.
[29] P. Roe, D. Balsara, Notes on the eigensystem of magnetohydrodynamics, SIAM J. Appl. Math. 56 (1996) 57–67.
[30] K. Sankaran, Simulation of MPD flows using a flux-limited numerical method for the MHD equations, Princeton Thesis of Master of Science in Engineering, 2001.
[31] E.M. Schneiter, P.F. Velázquez, A. Esquivel, A. Raga, X. Blanco-Cano, Three-dimensional hydrodynamical simulation of the exoplanet HD 209458b, Astrophys. J. 671 (1) (2007) L57–L60.
[32] S.A. Serna, Characteristic-based nonconvex entropy-fix upwind scheme for the ideal magnetohydrodynamic equations, J. Comput. Phys. 228 (11) (2009) 4232–4247.
[33] J.S. Shang, Recent research in magneto-aerodynamics, Prog. Aerospace Sci. 37 (2001).
[34] L. Spitzer, Physics of Fully Ionized Gases, Interscience, New York, 1956.
[35] G.W. Sutton, A. Sherman, Engineering Magnetohydrodynamics, McGraw–Hill, New York, 1965.
[36] E.F. Toro, Riemann Solvers and Numerical Methods for Fluid Dynamics, 2nd ed., Springer-Verlag, Germany, 1999.
[37] G. Tóth, The $\nabla \cdot \boldsymbol{B} = 0$ constraint in shock-capturing magnetohydrodynamics codes, J. Comput. Phys. 161 (2000) 605–652.
[38] B. Udrea, An advanced implicit solver for MHD, PhD thesis, University of Washington, 1999.
[39] B. Van Leer, W.T. Lee, K.G. Powell, Sonic-point capturing, in: Proc. 9th Computational Fluid Dynamics Conference, New York, USA, 1989, AIAA Paper 89-1945-CP.
[40] H. Yee, R. Warming, A. Harten, Implicit total variations diminishing (TVD) schemes for steady-sate calculations, J. Comput. Phys. 57 (1985) 327–360.
[41] H. Yee, A class of high-resolution explicit and implicit shock-capturing methods, NASA Technical Memorandum 101008, Ames Research Center, California, 1989.
[42] A. Zachary, A. Malagoli, P. Colella, A higher order Godunov method for multidimensional ideal magnetohydrodynamics, SIAM J. Sci. Comput. 15 (1994) 263–284.